Ben Gurion University
Faculty of Natural Sciences
Department of Physics

Zero-Temperature Phase Transitions of $LiHo_xY_{1-x}F_4$ in the Presence of Random Fields

Tomer Dollberg

supervised by
Prof. Moshe Schechter

October 16, 2017

Abstract

$LiHo_xY_{1-x}F_4$ under transverse magnetic field is considered a good realization of a disordered random field Ising model with long-range interactions. A ferromagnetic (FM) to quasi-spin glass (QSG) phase transition has been found to exist at random fields considerably smaller than the typical interaction strength between the spins for significant dilutions ($x < 0.6$) at zero temperature. This phase transition is studied using jaded extremal optimization to find ground states and finite-size scaling analysis is performed to find the phase transitions as a function random field strength at zero temperature.

Contents

1. Introduction

Random disorder is prevalent in many real-world physical systems and has been the subject of much research in the past few decades. In particular, some magnetic systems have proven to be well described by models that explicitly take into account the effects of random disorder. The model discussed in this work is the random-field Ising model (RFIM) which is an extension of the classical Ising model with a local longitudinal magnetic field that is random in both magnitude and sign. This model has been under theoretical investigation since the mid 1970s and as it turns out, the material $LiHo_xY_{1-x}F_4$ was found to be a very good real-world realization of said model [GH11, Sch08]. The questions investigated with relation to the RFIM are both those of classical phase transitions, which occur at non-zero temperature, and those of quantum phase transitions that may occur at zero temperature. A transition of the second sort is the focus of this work.

The use of computer simulations in order to investigate thermodynamical systems is not a new concept by any means, but the constant improvement in available processing power enables us to study systems much more complex than before. In addition, the study of a zero-temperature phase transition proves to be somewhat more difficult than with non-zero temperatures as finding ground states for Ising systems is computationally quite hard [Mid04]. Thus, recent developments in heuristic algorithms as well as the increase in available computational power provide a good chance to study such systems.

1.1. $LiHo_xY_{1-x}F_4$

$LiHoF_4$ is a rare-earth compound in which only the Holmium ions, Ho^{3+}, are magnetic. $LiHoF_4$ forms a tetragonal structure as depicted in figure 1.1 with lattice constants $a = 5.175$Å and $c = 10.75$Å. There are 4 Ho^{3+} ions per unit cell which form a lattice with a basis with coordinates $(0, 0, \frac{1}{2})$, $(0, \frac{1}{2}, \frac{3}{4})$, $(\frac{1}{2}, \frac{1}{2}, 0)$ and $(\frac{1}{2}, 0, \frac{1}{4})$. The unfilled $4f$ orbitals of the Holmium ions are not very spatially extended which makes the exchange interaction relatively weak and makes the magnetic dipolar interactions the most prominent between pairs of different ions [GH11]. In addition, measurements done in the mid 1970s showed that $LiHoF_4$ has a highly anisotropic g-tensor. Hence $LiHoF_4$ is well modeled by the Ising model with dipolar interactions, the ground state of which depends on the lattice structure and sample shape. We will be discussing $LiHoF_4$ in the limit of infinitely long thin samples in which a ground state of uniform magnetization exists.

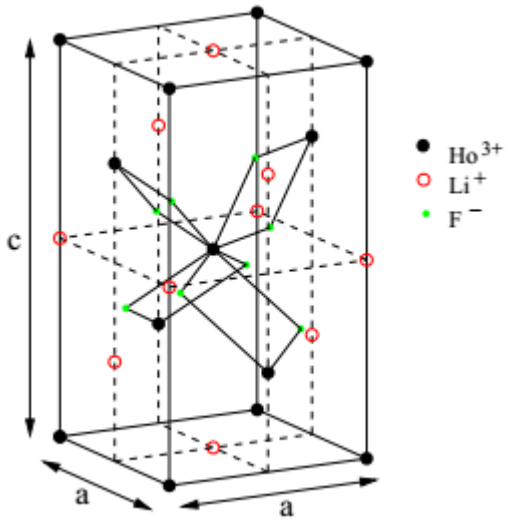

Figure 1.1. Crystalline tetragonal structure of $LiHoF_4$ with lattice spacing $a = 5.175$Å and $c = 10.75$Å. In $LiHo_xY_{1-x}F_4$, the magnetic Ho^{3+} ions are randomly substituted by non-magnetic Y^{3+} ions, with the lattice structure remaining the same for all x. The easy axis is along the c direction and a transverse magnetic field B_x is applied perpendicular to that axis in transverse field experiments[GH11].

The diluted variant of $LiHoF_4$ in which the magnetic Ho^{3+} ions are randomly substituted by Y^{3+} ions is referred to as $LiHo_xY_{1-x}F_4$ where x is a measure of the dilution, i.e. $x = 1$ would be regular $LiHoF_4$ and $x = 0$ would be a crystal with no Ho^{3+} ions at all, that is $LiYF_4$. The $LiHo_xY_{1-x}F_4$ forms a solid solution for all $x \in [0, 1]$ with no change to its crystalline structure and hence it enables us to model it as an Ising lattice with Y^{3+} occupied sites treated as vacant. For $0.3 < x < 1$, $LiHo_xY_{1-x}F_4$ can be described as a diluted ferromagnet [GH11, ATKS13]. The dipolar interactions, having a different sign depending on the displacement vector angle, are inherently frustrated. That is, some pairs of spins are forced to be in an energetically unfavorable orientation with each other as imposed by the ground state of the whole system. This is in contrast with, for example, a classic Ising ferromagnet, in which there exists a ground state where every pair of spins is in an energetically favorable configuration - that is when all spins are aligned. The disorder introduced by the substitution of Ho^{3+} with Y^{3+} makes this frustration random, and as x decreases we might expect the long range order to break down and for the ferromagnetic phase to be replaced by a spin-glass phase. This is indeed what was found to be happening as will be described later in this work.

1.2. Transverse field and random fields in $LiHo_xY_{1-x}F_4$

The RFIM has been under theoretical investigation for a long time, notably since its effect on the stability of the ordered state was discussed by Imry and

Ma in the mid 1970s. However, it was only in the last two decades or so that $LiHo_xY_{1-x}F_4$ was found to be a real world realization of the RFIM [Sch08]. Naively, a dipolar ferromagnet under a transverse field might be modeled by the transverse field Ising model (TFIM) as such [SL06]:

$$H = -\sum_{i,j} J_{ij}\tau_i^z\tau_j^z - \Delta\sum_i \tau_i^x \tag{1.1}$$

This captures the physics of a quantum phase transition (QPT) that might occur with a change of Δ and indeed $LiHo_xY_{1-x}F_4$ with $x = 1$ was shown to exhibit a ferromagnetic to paramagnetic QPT as a function of H_t at zero-temperature as well as the obvious phase transition as a function of temperature [SL06]. In this work we will be discussing transverse fields smaller than the critical H_t of the QPT, and instead we will study emergent random fields induced by the transverse field and the random spatial disorder.

The dipolar interaction in the $LiHo_xY_{1-x}F_4$ has the following form [GH11]

$$H_{dip} = \sum_{ij,\alpha\beta} V_{ij}^{\alpha\beta} J_i^\alpha J_j^\beta \tag{1.2}$$

where $\alpha, \beta = x, y, z$ and the dipolar interaction $V_{ij}^{\alpha\beta} = [\delta^{\alpha\beta}|\vec{r}_{ij}|^2 - 3(\vec{r}_{ij})^\alpha(\vec{r}_{ij})^\beta]/|\vec{r}_{ij}|^5$. In the case of $x = 1$, i.e. pure $LiHoF_4$, the off-diagonal terms in (1.2), e.g. $J_i^z J_j^x$, cancel out due to the symmetry of the lattice in addition to being effectively reduced [GH11, Sch08]. The application of a transverse magnetic field H_t and the introduction of dilution $x < 1$ makes the the sum of off diagonal terms not necessarily zero. This sum can then be regarded as an effective random local field interacting with the z component of the spin [SL06, Sch08] where the randomness of the field comes from the randomness of site occupancy via the term $\epsilon_i V_{ij}^{zx} \langle J_i^x \rangle$ where $\epsilon_i = \{0, 1\}$ is the occupation of the magnetic Ho^{3+} on the lattice site i. The relation between H_t, for $H_t \ll \Omega_0/(\mu_B S)$, and the random field is derived in reference [Sch08] and is as follows:

$$\tilde{h}_j = \frac{2SH_t}{\Omega_0}\sum_i \epsilon_i V_{ji}^{zx} \tag{1.3}$$

where $\Omega_0 \approx 10K$ is the measure of the anisotropy, given by the energy difference between each spin's ground state and its relevant excited state, and $S = 5.5$ is the magnitude of the effective Ho^{3+} spin. The random local energy is then given by the interaction of the local spin with this effective local field, $\tilde{\gamma}_j = \mu_B \tilde{h}_j S$. The important feature of the sum at 1.3 is that it is independent of the directions of the spins at sites i, which is what enables

us to treat it as a random quantity. This means that we can take the local random energy to be:

$$\gamma_j = \eta_j \frac{2\mu_B H_t S^2}{\Omega_0} V_0(1-x) \tag{1.4}$$

where V_0 is the magnitude of the dipolar interaction at a distance of one unit cell along the x direction, and η_j is a random number with $\langle \eta_j \rangle = 0$ and $Var(\eta_j)$ related to the dilution and calculated through a procedure described in reference [Sch08]. The consequence of this is that we may simulate the behavior of $LiHo_xY_{1-x}F_4$ in a transverse magnetic field as a dipolar magnet with local random longitudinal fields drawn from a random distribution with mean zero and variance $h \propto H_t$.

This means that, with the addition of nearest neighbor exchange interactions, the hamiltonian which describes $LiHo_xY_{1-x}F_4$ at low temperatures and in external transverse magnetic field is given by [ATKS13]

$$\mathcal{H} = \sum_{i \neq j} \frac{J_{ij}}{2} \epsilon_i \epsilon_j S_i S_j + \frac{J_{ex}}{2} \sum_{\langle i,j \rangle} \epsilon_i \epsilon_j S_i S_j + \sum_i h_i \epsilon_i S_i \tag{1.5}$$

where $S_i = \{\pm 1\}$, $J_{ij} = D(r_{ij}^2 - 3z_{ij}^2)/r_{ij}^5$ is the dipolar interaction with $D/a^3 = 0.214K$, $J_{ex} = 0.12K$ is the nearest neighbor exchange interaction, and h_i is drawn from a Gaussian distribution with zero mean and standard deviation h [ATKS13].

2. Numerical Methods

2.1. Extremal Optimization

We study the behavior of $LiHo_xY_{1-x}F_4$ in zero-temperature which is, in general, quite challenging due to the glassy dynamics and multiple metastable states which characterize disordered materials. The zero temperature forces us to find the ground state of the system which is a problem that cannot be computed in polynomial time in the system size for a 3D system [Mid04]. In the absence of an exact algorithm one is forced to use some kind of heuristic algorithm. One such algorithm which has proven to be quite efficient for the problem of the Ising spin glass is called Jaded Extremal Optimization (JEO) [Mid04] which is a variation of Extremal Optimization (EO) [BP01]. The extremal optimization algorithm is inspired by the phenomenon of self-organized criticality on which the Bak-Sneppen model of biological evolution is based [BP01]. The algorithm tries to find approximate solutions to optimization problems by continuously selecting against the least fit elements of the system without explicitly trying to improve them, thus having the optimal configurations arising naturally in the process.

In our case the different elements of the system are the spins in the configurations and the measure of the "fitness" of a single spin is its interaction with all other spins and the local random field in that site. We explicitly define the fitness of spin i (assuming site i is occupied) as

$$\lambda_i = -S_i\Big(\sum_j \frac{J_{ij}}{2}\epsilon_j S_j + \frac{J_{ex}}{2}\sum_{\langle i,j\rangle}\epsilon_j S_j + h_i\Big) \tag{2.1}$$

The minus sign in (2.1) makes sure that when improving the fitness of the spins we are lowering the energy of the system, since (2.1) is the energy of a single spin. We may also write the total energy of the system when it is in some configuration, s, as $E_{total}(s) = -\sum_i \lambda_i$. The basic outline of the EO algorithm is as follows:

1. Initialize random configuration s and set $s_{best} = s$.
2. For the current configuration s,
   a) Evaluate λ_i for each site S_i.
   b) Find the minimal λ_j out of all sites, i.e., the site with the worst fitness.
   c) Flip S_j such that a new configuration, s', is created.
   d) Accept $s = s'$ unconditionally.

e) If $E_{total}(s') < E_{total}(s)$ the set $s_{best} = s'$.

3. Repeat step 2 as long as desired.
4. Return s_{best} and $E_{total}(s_{best})$.

Focusing on the spin with the worst fitness in 2b leads to a deterministic process, leaving no choice in 2c. This process is likely to get stuck in metastable states, so to improve results a new parameter is introduced. Instead of step 2b, all spins are ranked according to fitness λ_i, such that the spin with the worst fitness is of rank 1 and the best is of rank n. Then we consider the probability distribution over the *ranks* k,

$$P_k \propto k^{-\tau},\ 1 \leq k \leq n \tag{2.2}$$

for a given value of the parameter τ. To finish the new step 2b we then choose a spin S_j according to P_k and continue to the next steps as listed. For $\tau \to \infty$ the process approaches the deterministic search initially presented, and for $\tau = 0$ the process is merely a random walk between states. Finite values of τ ensure that no rank gets completely excluded while still maintaining a bias towards flipping "bad" spins.

JEO is an extension of this algorithm that adjusts the fitness by an amount proportional to the number of times m_i that the site i has been previously chosen for a flip, that is,

$$\lambda_i \to \lambda_i + \Gamma m_i \tag{2.3}$$

where Γ is an "aging" parameter. The spins are sorted by this new λ_i and selected by rank according to (2.2) as usual. Setting $\Gamma = 0$ corresponds to the regular EO algorithm, but setting $\Gamma > 0$ reduces the probability of flipping spins that have been flipped many times before. The reasoning goes that in a glassy ground state, it is favorable for some spins to have low fitness so that a number of other spins may maximize their fitness. The introduction of $\Gamma > 0$ prevents these spins from being flipped in futility [Mid04].

Following references [Mid04] and [Boe05], some improvements were implemented into the JEO algorithm described above in order to speed it up. The most important of these are storing the spins in a heap structure, choosing a spin to flip from that heap in a manner that approximates (2.2), and dynamically ordering the heap as described in [Boe05].

2.2. Finite-size Scaling

A computer simulation is inherently limited by the available processing time and memory, and hence only finite systems may be simulated. We would still like to study the bulk characteristics of the system, which may be smeared

out for systems that are not infinitely large. The non-analytic part of a given observable can be described by a finite-size scaling form. For example, the finite-size magnetization from a simulation of an Ising system with L^d spins is asymptotically given by [Kat09]:

$$\langle m_L \rangle \sim L^{\beta/\nu} \tilde{M}[L^{1/\nu}(T - T_c)] \tag{2.4}$$

where $\tilde{M}$ is an unknown scaling function. (2.4) shows that data for $\langle m_L \rangle / L^{\beta/\nu}$ simulated for different system sizes L should all cross at $T = T_c$ as the argument of $\tilde{M}$ vanishes, so is independent of L. To use this argument we need to know β/ν which is not usually the case, so we would like to have a quantity other than $\langle m_L \rangle$ whose asymptotic behavior we might study. One such quantity is a dimensionless function known as the *Binder ratio*, and it is given by [Kat09, ATKS13]

$$g = \frac{1}{2}\left[3 - \frac{\langle m^4 \rangle}{\langle m^2 \rangle^2}\right] \sim \tilde{G}\left[L^{1/\nu}(x - x_c)\right] \tag{2.5}$$

where $\langle ... \rangle$ is a disorder average and $m = \frac{1}{N}\sum_i S_i$ is the magnetization density of the system. The factors in (2.5) ensure that $g \to 1$ for x$\to$1 and $g \to 0$ for $x \to 0$. Fitting g near the phase boundary allows for the extraction of x_c and ν [ATKS13].

2.3. Ewald Summation

As previously mentioned, we wish to simulate samples of $LiHo_xY_{1-x}F_4$ that are infinitely long, where a ground state of uniform magnetization exists. Of course, since a computer simulation is limited by processing time, only a finite system size may be simulated, and sizes larger than $L = 10$ (where L is the number of lattice unit cells in each direction) were not practical with the available processing power. Simulations are nonetheless effective when considering periodic boundary conditions that are characteristic of long, needle-shaped samples.

Initially, periodic boundary conditions were implemented naively, that is, for each pair of spins, the interaction that was considered was the interaction between the closest pair among all copies of both spins. Effectively, each spin was considered to be in the center of the sample in terms of its interactions with other spins. This method was unable to produce a ground state with uniform magnetization when the sample consisted of equal number of unit cells in each direction, as can be seen in figure 2.1. However, an elongated sample consisting of, for example, 3 times as many unit cells in the z direction as in the x and y directions does indeed have a ground state with uniform magnetization that is found with the JEO algorithm. Using actual

needle-shaped samples in simulations is quite resource consuming as many more spins need to be incorporated and a better method for simulating an infinitely long system is required.

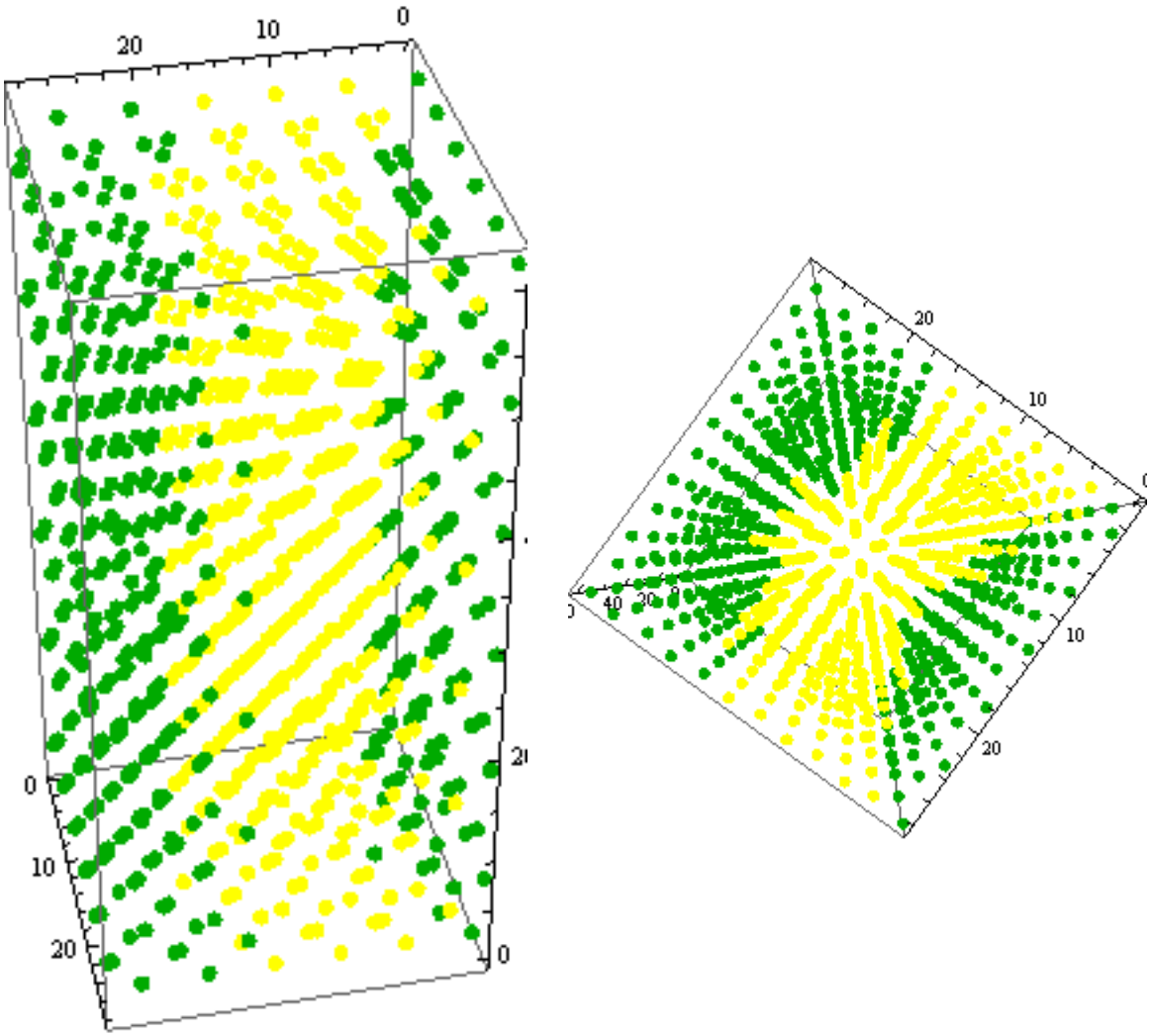

Figure 2.1. Ground state of $LiHoF_4$ with naively implemented boundary conditions and dipolar interactions. The sample is of size $L = 6$ and axes numbering is in Å. Green dots indicate spin down and yellow dots indicate spin up. A two-domain structure in this ground state is clearly visible, and indeed the magnetization of this state is $M = 0$. The left figure shows a side view of the sample and right figure shows a top view.

The method we chose to use is the Ewald summation method which is considered very useful for calculating long range dipolar interactions [SG09, GH11]. The sum we wish to calculate is

$$L_{ij}^{\mu\nu} = \sum_{\boldsymbol{n}}{}' \frac{\delta_{ij}(\boldsymbol{r}_{ij}+\boldsymbol{n})^2 - 3(\boldsymbol{r}_{ij}+\boldsymbol{n})^\mu(\boldsymbol{r}_{ij}+\boldsymbol{n})^\nu}{|\boldsymbol{r}_{ij}+\boldsymbol{n}|^5} \tag{2.6}$$

The prime symbol indicates that for $i = j$ the sum does not include the $\boldsymbol{n} = 0$ term. The sum in (2.6) is conditionally convergent, meaning that the result depends on the order of summation [SG09], which is why the Ewald method is required. In the Ewald method we separate this sum into two convergent sums: one in real space and the other in reciprocal space. A simplified derivation of the technique is presented in [SG09], here we shall only present the final forms used in this work:

$$L_{ij}^{\mu\nu} = \sum_{\boldsymbol{n}}{}' \frac{\delta_{\mu\nu}B(r_{ij})r_{ij}^2 - C(r_{ij})r_{ij}^\mu r_{ij}^\nu}{r_{ij}^5} + \frac{4\pi}{L^3}\sum_{\boldsymbol{K}\neq 0}\frac{K_\mu K_\nu}{K^2}e^{-K^2/4\alpha^2}e^{i\boldsymbol{K}\bullet\boldsymbol{r}_{ij}} - \frac{4\alpha^3}{3\sqrt{\pi}}\delta_{\mu\nu}\delta_{ij} \tag{2.7}$$

where

$$B(r) = erfc(r) + \frac{2\alpha r}{\sqrt{\pi}}e^{-\alpha^2 r^2} \tag{2.8a}$$

$$C(r) = 3erfc(r) + \frac{2\alpha r(3+2\alpha^2 r^2)}{\sqrt{\pi}}e^{-\alpha^2 r^2} \tag{2.8b}$$

$\boldsymbol{n} = L(k\hat{x} + l\hat{y} + m\hat{z})$ where k, l, m are integers and $\hat{x}, \hat{y}, \hat{z}$ are unit vectors and $\mathbf{K}$ are reciprocal lattice vectors. $erfc(x)$ is the complementary error function.

The first term in (2.7) is the real space sum, the second is the reciprocal space sum and the third is a self interaction correction term. Another term which accounts for the polarization of the surface may be introduced in order to model different system shapes, however for the case of a long, cylindrical shape which we are considering, this surface term is zero [SG09].

We calculate the real and reciprocal sums by truncating them at N_{cutoff}^{real} and $N_{cutoff}^{reciprocal}$ respectively. For the real sum, N_{cutoff}^{real} is the absolute value of the cutoff in each direction, so that in practice $(2N_{cutoff}^{real}+1)^3$ vectors are summed. $N_{cutoff}^{reciprocal}$ is the same for the reciprocal sum, but due to the symmetry of the sum and since we are only calculating L_{ij}^{zz}, only about half of the vectors need to be summed and the complex exponent may be replaced by a cosine. With

the exclusion of $\boldsymbol{K} = 0$, the total number of summed vectors turns out to be $(2N_{cutoff}^{reciprocal}+1)^2 \times N_{cutoff}^{reciprocal}$. Equation (2.7) is valid for any choice of α, but numerical convergence of the real and reciprocal sums depend strongly on the choice of α. Various references suggest values ranging between $\alpha = 1/L_z$ and $\alpha = 5/L_z$ so the convergence of the Ewald sum was studied in this range in order to decide the a suitable combination of α, N_{cutoff}^{real} and $N_{cutoff}^{reciprocal}$. The total energy of a checkers-board-like configuration was calculated and the energy per site as a function of α is plotted for various N_{cutoff}^{real} and $N_{cutoff}^{reciprocal}$ values in figure 2.2. A good parameter combination is one where the energy per site is constant as a function of α.

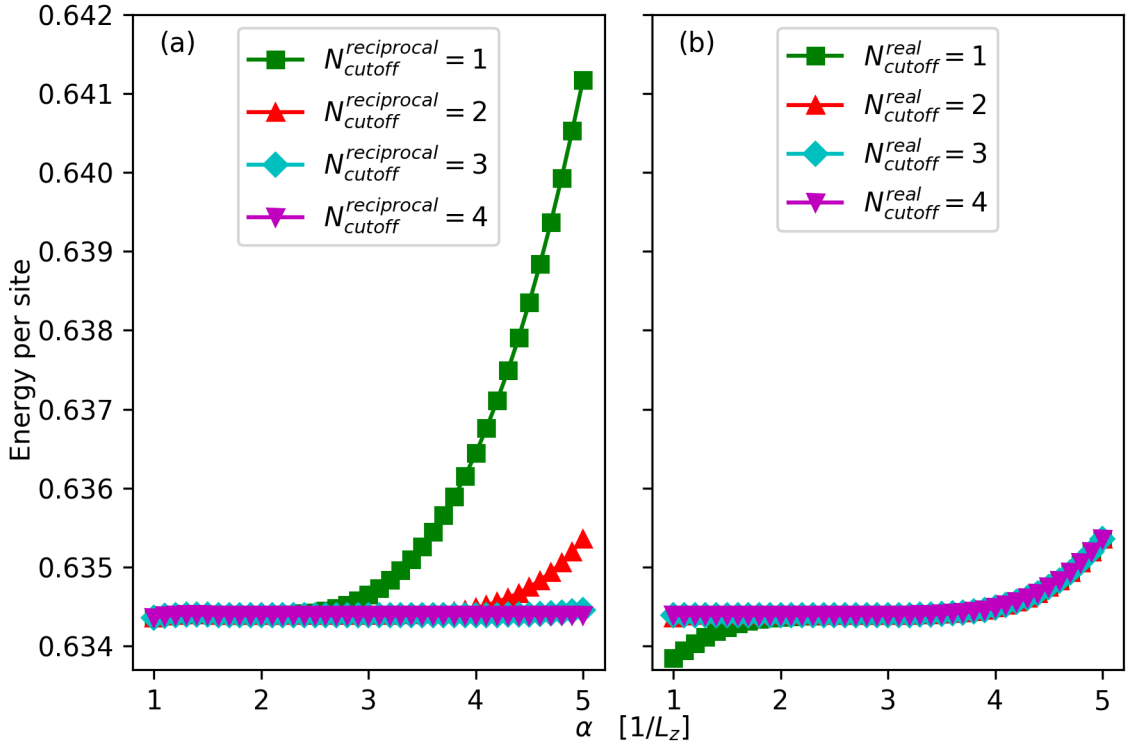

Figure 2.2. Energy per site as a function of α for a checkers-board-like system of size $L = 4$. (a) N_{cutoff}^{real} is held constant at 2 and (b) $N_{cutoff}^{reciprocal}$ is held constant at 2. These results shows that already at a cutoff of 4 for both sums there is good convergence to an α-independent value.

These results show that at a cutoff of $N_{cutoff} = 4$ for both sums there is already good convergence to a value which does not depend on α. Additional tests found that cutoffs of $N_{cutoff}^{reciprocal} = 6$ and $N_{cutoff}^{real} = 5$ give energy that is exactly constant, up to the computer's precision limit. As can be seen in figure 2.2, the α value for which the convergence is quickest is around $\alpha = 2$, and that is the value which was chosen for the simulations. The spins in this simulation never change their positions so the interactions between them change only in sign and never in magnitude during the simulation. As a result we can calculate the interactions once for each system size and save these to a file to be read at the beginning of each run. This makes processing time less of a concern which allows us to set $N_{cutoff}^{reciprocal} = 12$ and $N_{cutoff}^{real} = 10$.

3. Results

3.1. The Procedure

We wish to study the quasi-spin glass (QSG) to ferromagnetic (FM) phase transition of $LiHo_xY_{1-x}F_4$ as a function of x in zero-temperature and the dependence of the critical x_c on the characteristic magnitude of random local magnetic fields h. In particular we want to reproduce some of the results presented in [ATKS13] in figure 1.

The procedure we follow is very similar to the one presented in the paper mentioned above, with some changes that were dictated by available computational resources. The outline of the procedure is as follows:

1. We set the standard deviation of the local random fields h to a specific value.
2. Then, for each system size L:
   a) For each different $x \in [x_{min}, x_{max}]$ with step size Δx.
      i. Generate N_{sa} random disorder realizations with Ho^{3+} dilution x and local random fields of standard deviation h.
      ii. Find the ground state of each of the N_{sa} disorder realizations using JEO.[1]
      iii. Calculate the magnetization of each of the ground states.
      iv. Calculate the Binder ratio based on the averages of the N_{sa} systems.
   b) Fit a 3^{rd} order polynomial to the Binder ratio g as a function of x.
3. Find the point at which the curves of all system sizes cross. This is the critical dilution x_c at which the phase transition occurs.

We repeat the above procedure for different h and that should enable us to plot a $h - x$ phase diagram. Two values of h were studied within the scope of this project, $h = 0$ and $h = 0.05$. Details of the numerical simulations are presented in section §3.2.

3.2. Numerical details and parameters

Parameters and numerical details are presented below.

[1] Each disorder realization undergoes at least 10 independent runs starting from different initial configurations. Out of the supposed ground states found in each of the runs, the state with the lowest energy is assume to be the real ground state. This procedure is further discussed in section §3.4

Systems of sizes $L = 4, 6, and 8$ were studied. $x_{min}(x_{max})$ is the smallest (largest) dilution studied and Δx is the step size between measurements.

Each disorder realization underwent N_{valid} independent runs of the JEO algorithm to find N_{valid} ground states. The purpose of this was to establish the validity of the found ground states by setting a criterion for the minimal percentage of runs in which the same ground state had been found. Eventually, due to time constraints N_{valid} was set to 10 for most of the runs which is too small a sample to infer from about the validity of the results. Nevertheless the number of independent runs still acts to improve the validity of the results since starting from different initial configurations gives a better chance at finding the real ground state as opposed to a low energy metastable state. N_{valid} was equal to 100 for $x = 0.28$, 0.29 and $L = 4$, and $N_{valid} = 10$ for all other runs.

The two parameters of JEO were set to $\tau = 1.6$ and $\Gamma = 0.05$ following reference [ATKS13] for all runs.

N_{JEO} is the number of steps the JEO algorithm was run on each disorder realization, as described in step 3 on page 8.

h	x_{min}	x_{max}	Δx	N_{sa}
0	0.28	0.35	0.01	5000
0.05	0.3	0.4	0.025	2000-3000

Table 3.1. Simulation parameters for zero-temperature phase transition calculations. h is the standard deviation of the random local magnetic fields, $x_{min}(x_{max})$ is the smallest (largest) dilution studied and Δx is the step size between measurements. N_{sa} is the number of disorder realizations studied at each x.

L	x	N_{JEO}	N_{valid}	L	x	N_{JEO}	N_{valid}	L	x	N_{JEO}	N_{valid}
4	0.28	2^{26}	100	6	0.28	2^{26}	10	8	0.28	2^{27}	10
	0.29		100		0.29				0.29		
	0.3		10		0.3				0.3		
	0.31				0.31				0.31		
	0.32				0.32				0.32		
	0.33				0.33				0.33		
	0.34				0.34				0.34		
	0.35				0.35				0.35		

Table 3.2. Numerical details for $h = 0$ simulations. x is the Ho^{3+} concentration, N_{JEO} is the number of JEO steps run on each disorder realization and N_{valid} is the number of independent JEO runs on each disorder realization.

Initially the results for $h > 0$ were not as expected, meaning the findings of [ATKS13] were not reproduced. This led to the realization that for systems with $h > 0$ the finding of the ground state is significantly more difficult than for $h = 0$ and so a new criterion was introduced. Instead of specifying N_{JEO} initially based on a few sample tests, N_{JEO} was to be determined during

each run according to the following criterion: within the range $2^{26} - 2^{29}$ JEO steps, the program stops when the number of JEO steps since the last time a new minimal energy was found is equal to half the total JEO steps run thus far. In other words, if a minimal energy state is found at step n, and no *new* energy state is found in the next n steps, the program stops, as long as the total number of steps $2n$ is within the range $2^{26} - 2^{29}$. This gives a good measure of the real-time equilibration of the algorithm, and has indeed produced better results. N_{JEO} thus varies between runs and the average values are presented below.

L	x	$\overline{N_{JEO}}$	N_{sa}	N_{valid}
4	0.3	2^{26}	3000	10
	0.325			
	0.35			
	0.375		2000	
	0.4			
L	x	$\overline{N_{JEO}}$	N_{sa}	N_{valid}
6	0.3	2^{26}	3000	10
	0.325			
	0.35			
	0.375		2000	
	0.4			
L	x	$\overline{N_{JEO}}$	N_{sa}	N_{valid}
8	0.3	9.2×10^7	3000	10
	0.325	8.6×10^7		
	0.35	7.8×10^7		
	0.375	7.3×10^7	2000	
	0.4	7×10^7		

Table 3.3. Numerical details for $h = 0.05$ simulations. x is the Ho^{3+} concentration, N_{JEO} is the number of JEO steps run on each disorder realization and N_{valid} is the number of independent JEO runs on each disorder realization.

3.3. Binder ratio vs. x

The results for the two values of h studied are presented in the following figures.

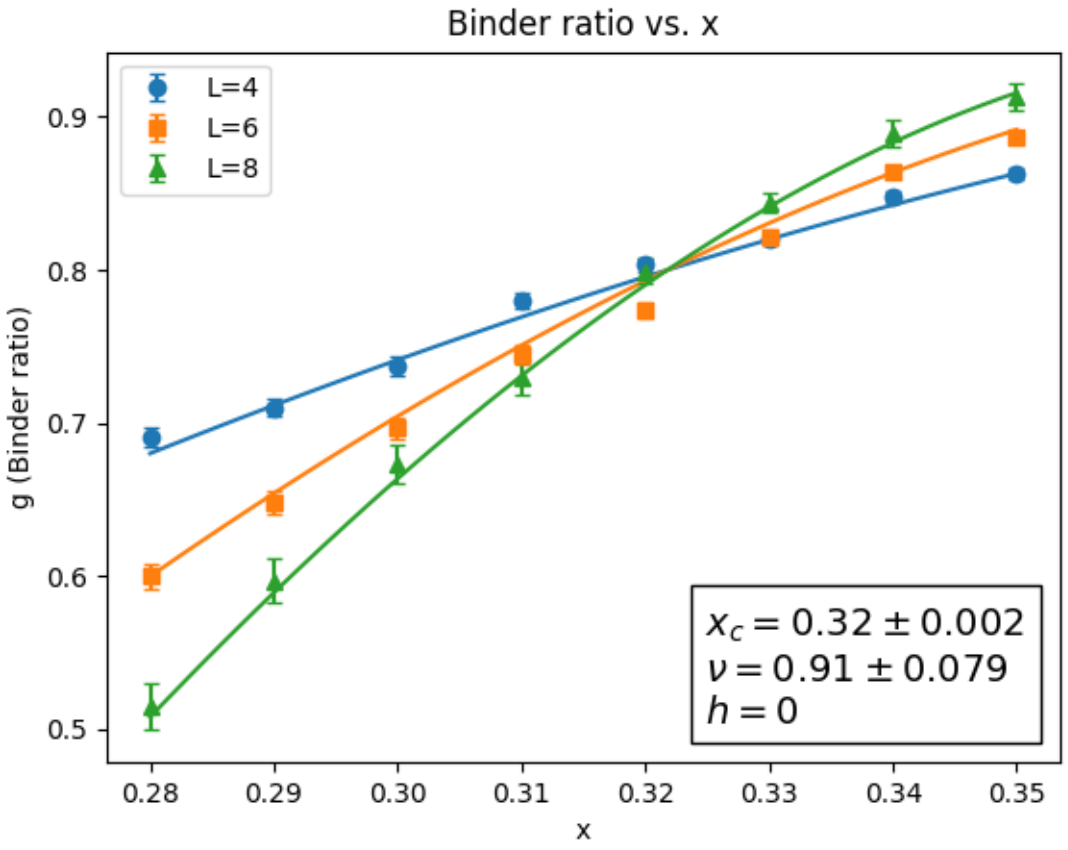

Figure 3.1. Binder ratio as a function of Ho^{3+} concentration x for three system sizes $L = 4$, 6, *and* 8 at $h = 0$. The crossing is found to be $x_c = 0.32 \pm 0.002$.

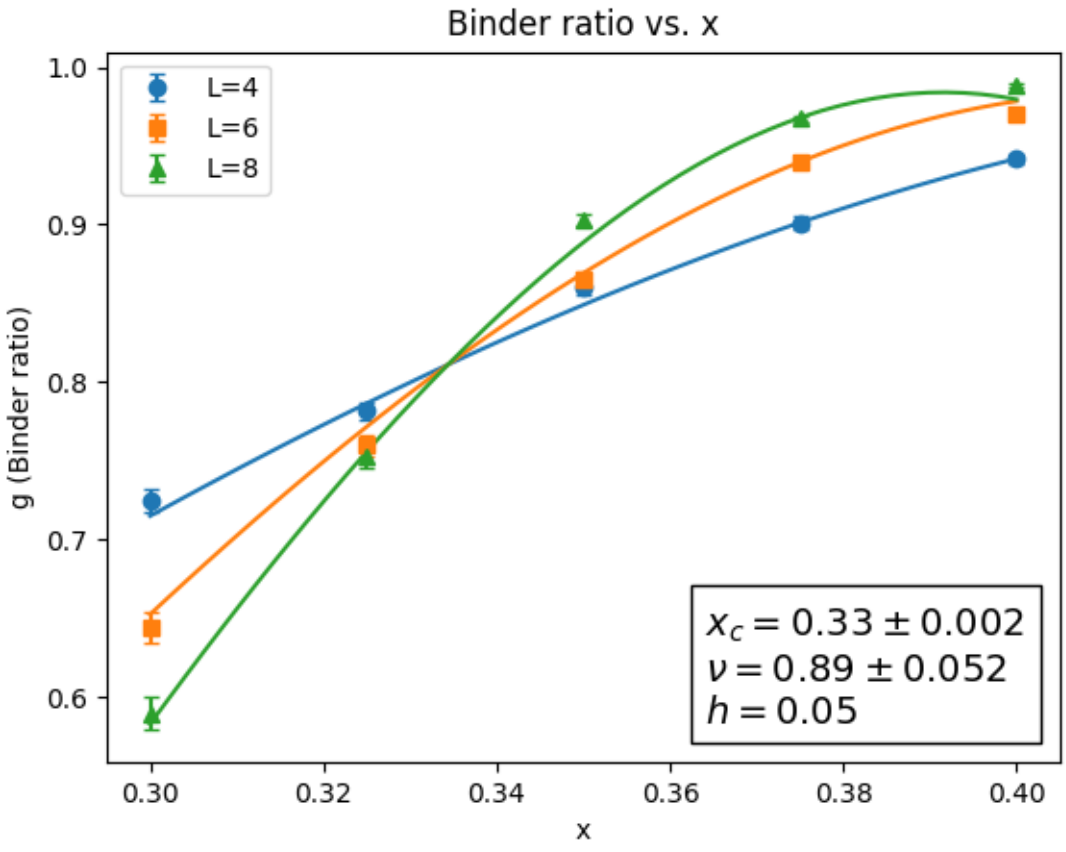

Figure 3.2. Binder ratio as a function of Ho^{3+} concentration x for three system sizes $L = 4$, 6, *and* 8 at $h = 0.05$. The crossing is found to be $x_c = 0.33 \pm 0.002$.

We assume that equation (2.5) can be approximated by a 3rd order polynomial, $\tilde{G}(z) = p_0 + p_1 z + p_2 z^2 + p_3 z^3$ where $z = L^{1/\nu}(x - x_c)$. Hence we perform a least square fit (using the Levenberg–Marquardt algorithm) for all three system sizes simultaneously, with the parameters p_0, p_1, p_2, p_3, ν and x_c being shared between fits. This ensures that the three curves meet at some point x_c. A more robust method of finding x_c which was not used here is discussed in section §3.4.

Error bars are determined using the bootstrap method as follows: For each system size L and N_{sa} disorder realizations, we randomly select N_{sa} samples (with repetition) for each value of x to create a new data set from which we calculate the Binder ratio. We repeat this process $N_{boot} = 500$ times, and then for each of the new data sets we perform a fit as described above. This gives us N_{boot} estimates of the fit parameters and the error of these is simply the standard deviation among the N_{boot} bootstrap estimates [KKY06]. The data points plotted in figure 3.1 and in figure 3.2 are the averages of these N_{boot} samples.

3.4. Discussion

The final results obtained in the course of this project and presented in this work, although similar to the results published in [ATKS13], are not identical. Specifically, the results published in [ATKS13] have the $h = 0$ phase transition at $x = 0.3$ and the $h = 0.05$ phase transition at $x \approx 0.35$ while the results presented here have the former at $x = 0.32 \pm 0.002$ and the latter at $x = 0.33 \pm 0.002$.

Since the procedure employed in this work is very similar to the one used in [ATKS13], this difference needs to be addressed. We would like to suggest three significant differences between the two procedures that most likely impacted our results.

— Due to time and resource constraints we were unable to employ the same level of robustness in validating the ground states. The number of independent JEO runs used in [ATKS13] was $N_{valid} = 512$ compared with our $N_{valid} = 10$ in most cases. This means we cannot confidently say that the ground states found using the JEO algorithm are the real ground states of the system, and they might be metastable states. This is important since the disordering mechanism described in [ATKS13] requires the flipping of domains of spins which might create hard-to-find ground states.
— This work used smaller system sizes than the ones used in [ATKS13], specifically $L = 4, 6\,and\,8$ compared with $L = 6, 8\,and\,10$. Smaller system sizes add more finite size corrections which probably affected our results. A better way of doing the finite size scaling, had more system sizes been available, would have been to find crossing points between two successive system size pairs (e.g. L and $2L$) and to analyze the convergence of the series of crossing points as $L \to \infty$ [Kat09]. This was not

feasible with only 3 system sizes, but for $h = 0$, when fitting simultaneously only $L = 4, 6$ and then $L = 6, 8$ the results where respectively $x_c = 0.33 \pm 0.002$ and $x_c = 0.31 \pm 0.003$, so the trend seems to be in the right direction. These fits are presented in chapter 4.

— We used the JEO parameters $\tau = 1.6$ and $\Gamma = 0.05$ similar to what is reported in [ATKS13]. However, [ATKS13] used a number of τ values (1.6, 1.8 and 2) whereas we only used one. Again, time constraints prevented us from further optimizing the parameters we used, which might have enabled us to get better results, either by directly improving the precision of the algorithm or by speeding up the process and thus enabling more samples to be simulated.

Another concerning issue is that the errors calculated in this work are about an order of magnitude *smaller* than the errors in [ATKS13], specifically in the case of $h = 0.05$. This issue in currently being discussed with J. C. Andresen to find out if there is a problem with the error calculation procedure or with anything else done in this project.

In any case, the results obtained, though not as accurate as previous published results, provide a basic proof of the validity of the current implementation of the procedure and algorithm.

4. Appendix A

Fitting of only pairs of system sizes are presented below.

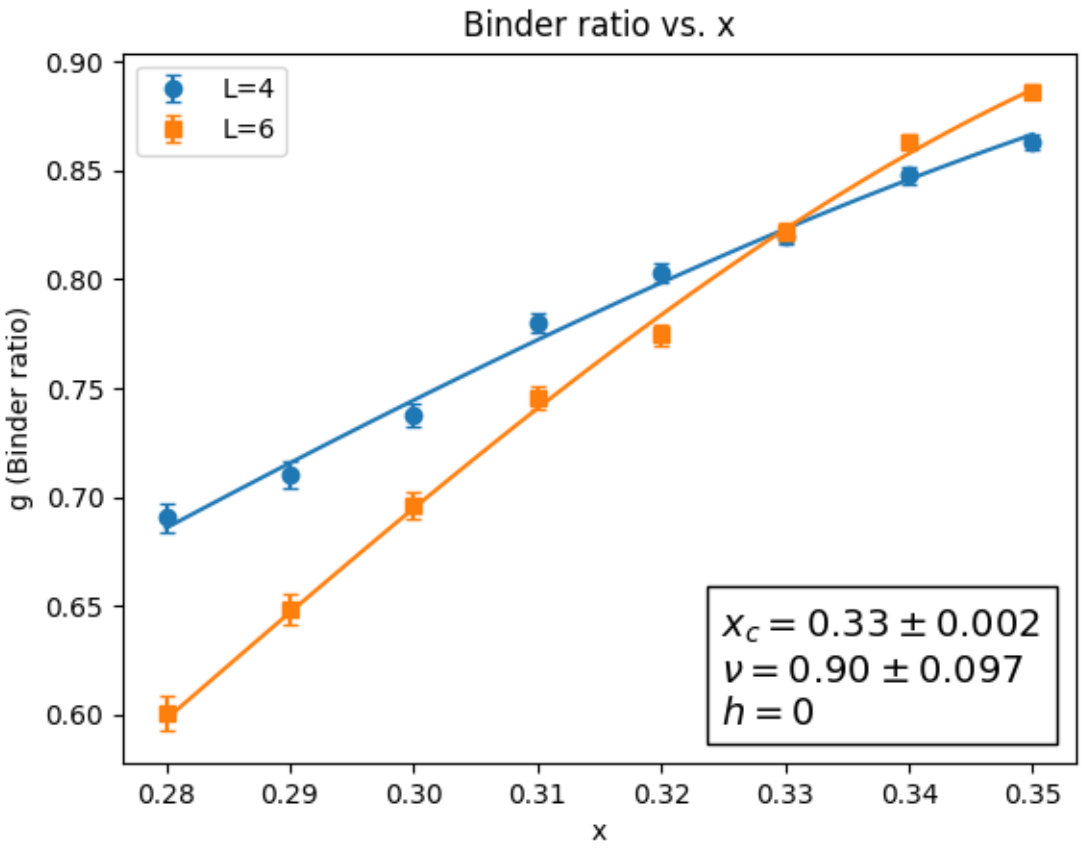

Figure 4.1. Binder ratio as a function of Ho^{3+} concentration x for *two* system sizes $L = 4, 6$ at $h = 0$. The crossing is found to be $x_c = 0.33 \pm 0.002$.

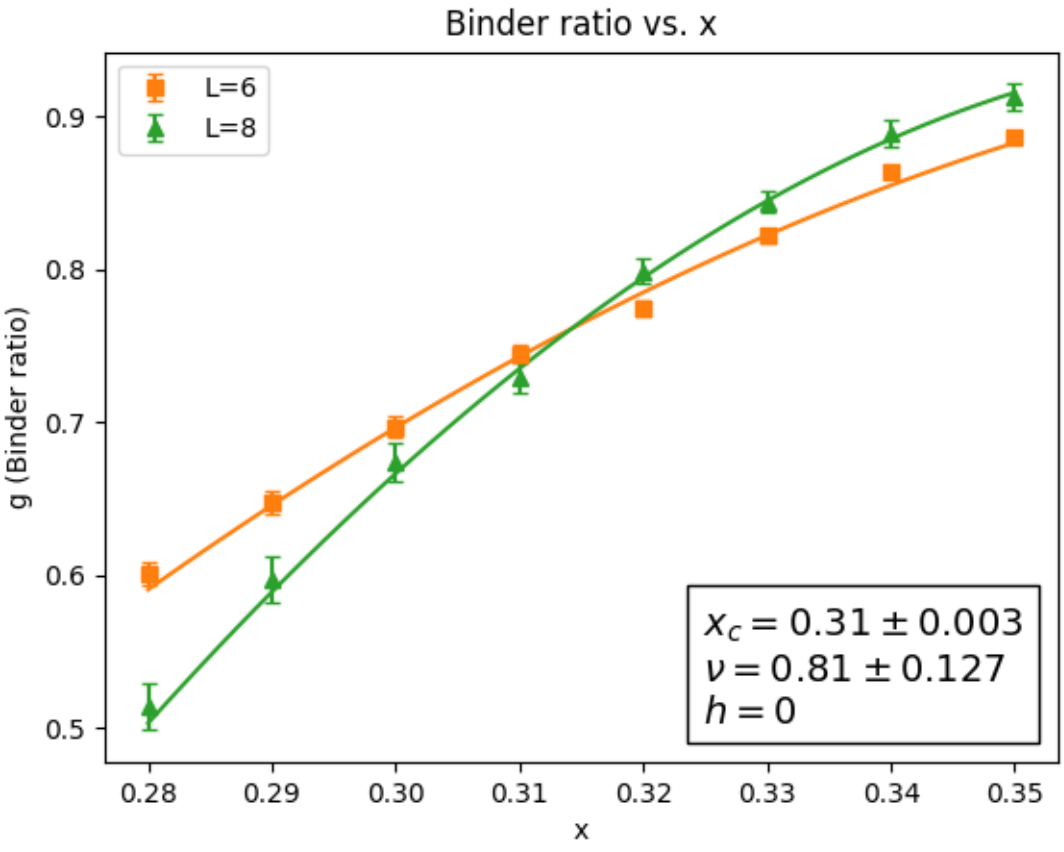

Figure 4.2. Binder ratio as a function of Ho^{3+} concentration x for *two* system sizes $L = 6, 8$ at $h = 0$. The crossing is found to be $x_c = 0.31 \pm 0.003$.

Bibliography

[ATKS13] Juan Carlos Andresen, Creighton K. Thomas, Helmut G. Katzgraber, and Moshe Schechter. Novel disordering mechanism in ferromagnetic systems with competing interactions. *Phys. Rev. Lett.*, 111: 177202, Oct 2013, https://link.aps.org/doi/10.1103/PhysRevLett.111.177202.

[Boe05] S. Boettcher. Extremal optimization for sherrington-kirkpatrick spin glasses. *The European Physical Journal B - Condensed Matter and Complex Systems*, 46(4): 501–505, Aug 2005, https://doi.org/10.1140/epjb/e2005-00280-6.

[BP01] Stefan Boettcher and Allon G. Percus. Optimization with extremal dynamics. *Phys. Rev. Lett.*, 86: 5211–5214, Jun 2001, https://link.aps.org/doi/10.1103/PhysRevLett.86.5211.

[GH11] Michel J P Gingras and Patrik Henelius. Collective phenomena in the liho x y 1-x f 4 quantum ising magnet: Recent progress and open questions. *Journal of Physics: Conference Series*, 320(1): 012001, 2011, http://stacks.iop.org/1742-6596/320/i=1/a=012001.

[Kat09] H.G. Katzgraber. Introduction to Monte Carlo Methods. *ArXiv e-prints*, May 2009, http://adsabs.harvard.edu/abs/2009arXiv0905.1629K.

[KKY06] Helmut G. Katzgraber, Mathias Körner, and A. P. Young. Universality in three-dimensional ising spin glasses: A monte carlo study. *Phys. Rev. B*, 73: 224432, Jun 2006, https://link.aps.org/doi/10.1103/PhysRevB.73.224432.

[Mid04] A. Alan Middleton. Improved extremal optimization for the ising spin glass. *Phys. Rev. E*, 69: 055701, May 2004, https://link.aps.org/doi/10.1103/PhysRevE.69.055701.

[Sch08] Moshe Schechter. $\mathrm{liho}_x\mathrm{y}_{1-x}\mathrm{f}_4$. *Phys. Rev. B*, 77: 020401, Jan 2008, https://link.aps.org/doi/10.1103/PhysRevB.77.020401.

[SG09] P. Stasiak and M. J. P. Gingras. Evidence for a Finite-Temperature Spin Glass Transition in a Diluted Dipolar Heisenberg Model in Three Dimensions, Appendix C. *ArXiv e-prints*, December 2009, https://arxiv.org/abs/0912.3469.

[SL06] Moshe Schechter and Nicolas Laflorencie. Quantum spin glass and the dipolar interaction. *Phys. Rev. Lett.*, 97: 137204, Sep 2006, https://link.aps.org/doi/10.1103/PhysRevLett.97.137204.